Available online at www.sciencedirect.com
SCIENCE DIRECT
Polymer 47 (2006) 1749–1754
polymer
www.elsevier.com/locate/polymer

SOS||TDDFT study on the dynamic third-order nonlinear optical properties of aniline oligomers based on the optimized configurations

Fei-Fei Li, Dong-Sheng Wu, You-Zhao Lan, Juan Shen, Shu-Ping Huang, Wen-Dan Cheng *, Hao Zhang, Ya-Jing Gong

State Key Laboratory of Structural Chemistry, The Graduate School of the Chinese Academy of Sciences, Fujian Institute of Research on the Structure of Matter, Fuzhou, Fujian 350002, People's Republic of China

Received 15 November 2005; received in revised form 27 December 2005; accepted 3 January 2006
Available online 24 January 2006

Abstract

In this paper, we employ the sum-over-states formula to calculate the dynamic third-order nonlinear optical polarizabilities of three optical processes, third-harmonic generation, electric-field-induced second-harmonic generation, and degenerate four-wave mixing, at the ground state of aniline oligomers. The ground state configurations of these compounds are obtained by the geometrical optimizations based on the B3LYP/6-31G** level. The transition moment elements and the transition energies are obtained by using the time-dependent density functional theory at the B3LYP/6-31G* level. The calculated results show that the third-order polarizability $\langle\gamma\rangle$ at the ground singlet state is increasing with the increase of repeat units number N of aniline oligomers and it approaches saturation at chain length around $N=7$–8.

Keywords: DFT; SOS method; Polarizability

1. Introduction

Conjugated organic molecules have attracted much attention during the last decade for their nonlinear optical properties, both for a fundamental point of view and for their potential application in optical data processing [1]. Recently, a number of studies have focused on their large third-order susceptibilities, $\chi^{(3)}$, ranging from 10^{-12} to 10^{-9} esu, and response time of few picoseconds or shorter [2–5]. In addition, it was observed that the third-order polarizability γ and the nonlinear susceptibility $\chi^{(3)}$ increase with the extent of the polymer backbone [6,7]. The calculated hyperpolarizabilities of quasilinear organic molecules were reported to be overestimated by the conventional DFT method [8–11], and a major improvement for the calculation of nonlinear optical properties was reported by the time-dependent current–density-functional theory [12,13].

Among the most studied conjugated polymers (CP), polyaniline was a unique example due to its high conductivity and chemical stability at ambient conditions. In the past, the studies of polyaniline were mainly focused on the structure, electronic properties [14] and magnetic properties [15] of aniline oligomers. Very little experimental data and theoretical study on the hyperpolarizability have been published [16] for extended polyaniline molecules. A number of theoretical studies were devoted to chain-length saturation of polyenes. The results consistently indicated that the saturation sets in after 50–60 carbons [7,17,18]. Beljonne et al. [19] investigated the saturation behavior in oligothiophenes using the semiempirical Austin Model 1 (AM1) techniques to estimate geometries and using an intermediate neglect of differential overlap/configuration interaction (INDO/CI) techniques to calculate electronic transition energies. The calculated results indicated that the saturation behavior in oligothiophenes occurs after 7–8 rings, as is in an excellent agreement with the experimental data of Prasad and co-workers [20]. Humphrey et al. [21] investigated the second hyperpolarizability of ethynyl-linked azobenzene molecular wires and find that the hyperpolarizability γ data could be described using a power law of $\gamma=\gamma_m n^{2.12\pm0.05}$ for oligomers with $n=2$–36 and while $n=55$ and 150 oligomers deviate from this power law due to the expected saturation effects. To our knowledge, no theoretical study of the length dependence of γ for aniline oligomers has been published, in which both conformational and electron-correlation effects are taken into account.

* Corresponding author. Tel.: +86 591 837 13068; fax: +86 591 837 14946.
E-mail address: cwd@fjirsm.ac.cn (W.-D. Cheng).

0032-3861/$ - see front matter © 2006 Elsevier Ltd. All rights reserved.
doi:10.1016/j.polymer.2006.01.002

In this study, we will report the optimized configurations of the aniline oligomers (from $N=1$ to 8) based on the density functional theory. Then, we will calculate the dynamic third-order optical polarizabilities in terms of the sum-over-states method combined with the time-dependent density functional theory (SOS||TDDFT). Finally, we will give the relationship between the length of the conjugation chain and the third-order polarizabilities for aniline oligomers (from monomer to ocxamer).

2. Computational procedures

The geometrical optimizations of the polyaniline (from monomer to octamer) are carried out at the B3LYP/6-31G** level using DFT method of the GAUSSIAN 98 program [22]. During the optimized processes, a convergent value of RMS (room-mean-square) density matrix and the critical values of force and displacement are set by default of the GAUSSIAN 98 program. Hence a stationary point of minimum on energy surfaces corresponds to equilibrium of these aniline oligomers. The all studied aniline oligomers have no symmetry.

Then the frequency-dependent third-order nonlinear optical polarizabilities are calculated by using the TDDFT method [23] at B3LYP model with 6-31G* basis sets combined with sum-over-states (SOS) method [24,25]. Here, the calculation of γ only concerns the state dipole moments and state–state transition moments depending on the molecular geometry and state function, and state energy based on the SOS method. The dipole moments, transition moments, and energies of states obtained by TDDFT method are taken as the inputs of SOS formula in this work. The average third-order polarizability is obtained by:

$$\langle\gamma\rangle = \frac{1}{5}(\gamma_{xxxx} + \gamma_{yyyy} + \gamma_{zzzz} + \gamma_{xxyy} + \gamma_{xxzz} + \gamma_{yyxx} + \gamma_{yyzz} + \gamma_{zzxx} + \gamma_{zzyy}) \quad (1)$$

And polarizability component γ_{abcd} is calculated by this formula:

$$\gamma_{abcd}(-\omega_p;\omega_1,\omega_2,\omega_3) = \left(\frac{2\pi}{h}\right)^3 K(-\omega_p;\omega_1,\omega_2,\omega_3)e^4 \left\{\sum_P\left[\sum_{i,j,k}{}' \frac{\langle 0|r_a|k\rangle\langle k|r_b^*|j\rangle\langle j|r_c^*|i\rangle\langle i|r_d|0\rangle}{(\omega_{k0}-\omega_p)(\omega_{j0}-\omega_1-\omega_2)(\omega_{i0}-\omega_1)}\right] - \sum_P\left[\sum_{j,k}{}' \frac{\langle 0|r_a|j\rangle\langle j|r_b|0\rangle\langle 0|r_c|k\rangle\langle k|r_d|0\rangle}{(\omega_{j0}-\omega_p)(\omega_{j0}-\omega_1)(\omega_{k0}+\omega_2)}\right]\right\} \quad (2)$$

Hereafter the mark $\gamma(3\omega)$, $\gamma(2\omega)$, and $\gamma(\omega)$ symbolizes the third-order polarizability of the third-harmonic generation (THG) of $\gamma(-3\omega;\omega,\omega,\omega)$, electric-field-induced second-harmonic generation (EFISHG) of $\gamma(-2\omega;\omega,\omega,0)$, and degenerate four-wave mixing (DFWM) of $\gamma(-\omega;\omega,\omega,-\omega)$, individually. The prefactor $K(\omega_p;\omega_1,\omega_2,\omega_3)$ must be taken as the same value in the THG, EFISHG, and DFWM process for the static case of an input photon energy of zero, and it is the relative magnitude of the reference state nonlinear polarizability for each optical process at nonzero frequency. In the following calculation, we use the same prefactor K in order to make the remark to justify plotting curves for the nonlinear polarizabilities of three optical processes against common axes. In order to obtain a reliable value of γ, the time-dependent density functional theory at the TDB3LYP/6-31G* level is employed to calculate the state dipole moments, state–state transition moments and the transition energies. The linear and nonlinear polarizailities calculated by TDDFT method have been reported and the obtained results have been proved to be reliable [26–28].

3. Results and discussions

3.1. Geometrical structures

The geometrical structures of oligomers from monomer to octamer are optimized by using DFT method at B3LYP/6-31G** level. Fig. 1 only shows the optimized geometry of aniline trimer and pentamer and the numbering scheme of atoms. Some calculated bond lengths and angles of the aniline

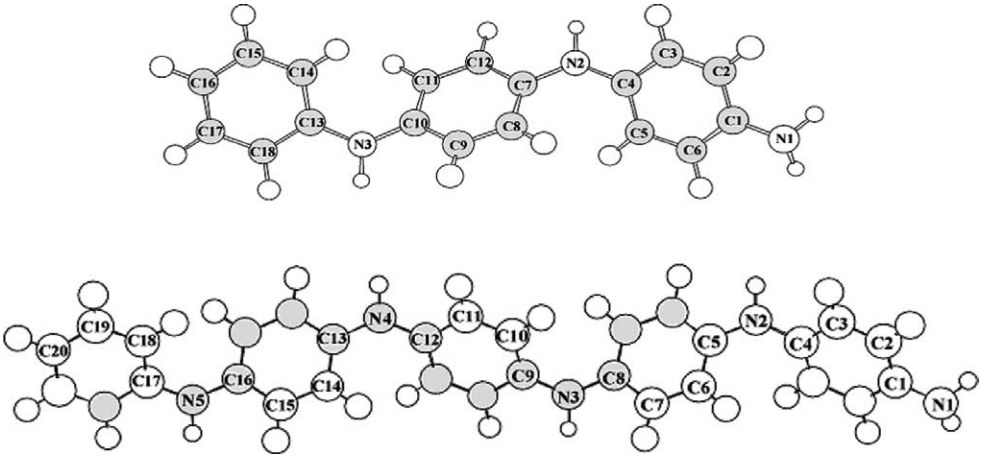

Fig. 1. Optimized geometrical structure of aniline trimer and pentamer and atomic numbering.

Table 1
Calculated bond lengths and bond angles and corresponding experimental values

Trimer			Pentamer		
Bond	B3LYP/6-31G**	Expt.	Bond	B3LYP/6-31G**	Expt.
Bond lengths (Å)					
C1–N1	1.403	1.399[a]	C1–N1	1.404	1.399[a]
C1–C2	1.394	1.385[a]	C1–C6	1.403	1.403[a]
C1–C6	1.404	1.403[a]	C2–C3	1.391	1.379[a]
C2–C3	1.391	1.379[a]	C5–C6	1.405	1.392[b]
C7–N2	1.398	1.395[c]	C6–C7	1.390	1.380[b]
C10–C11	1.405	1.397[c]	N1–H	1.012	1.069[a]
C11–C12	1.390	1.386[c]	N2–H	1.008	0.819[b]
N2–H	1.008	0.846[c]			
Bond angles (°)					
H–N1–H	110.7	110.1[a]	H–N1–H	110.7	110.1[a]
C6–C1–N1	122.0	122.0[a]	C2–C1–N1	122.0	122.0[a]
N2–C4–C5	122.5	122.3[c]	C1–C2–C3	121.3	121.8[a]
C8–C7–N2	123.4	124.2[c]	C4–N2–C5	128.7	127.6[b]
C7–C2–H	115.3	116.0[c]	C5–N2–H	115.6	114.8[b]
N2–C4–C3	119.5	120.5[c]	N2–C5–C6	123.2	123.5[b]
Dihedral angles (°)					
N1–C1–C2–C3	−175.99	−174.63[a]	N1–C1–C2–C3	−176.0	−174.6[a]
N2–C7–C8–C9	178.21	177.51[c]	C3–C4–N2–C5	−150.4	−154.2[b]
C18–C13–N3–H	−19.25	−16.83[c]	C6–C5–N2–C4	22.0	25.1[b]
C11–C10–C13–C14	−44.16	−42.06[c]	C6–C5–C4–C3	−119.2	−121.4[b]

[a] Ref. [29].
[b] Ref. [31].
[c] Ref. [30].

trimer and pentamer are listed in Table 1, together with the experimental values [29–31] of related aniline oligomers. For trimer, the bond lengths of C1–N1 and C7–N2 are 1.403 and 1.398 Å, and the corresponding experimental values of bond lengths are 1.399 and 1.395 Å, respectively. The range of C–C bonds is from 1.390 to 1.405 Å and falls well between single bond (1.54 Å) and double bond (1.34 Å). The benzene rings between neighbors in the aniline trimer have a little twist, and the configuration has a large scroll along with molecular chain as the number of benzene ring increases. The dihedral angles of N2–C7–C8–C9, C11–C10–C13–C14 and C18–C13–N3–H are 178.21, −44.16 and −19.25°, and the corresponding experimental values are 177.51, −42.06 and −16.83°, respectively. It is shown that the calculated values are in agreement with the experimental data and the optimized structures are reliable. For other aniline oligomers, the optimized geometrical parameters are similar to those of the trimer and pentamer.

The calculated Mulliken populations at ground state for the aniline monomer, tetramer and heptamer are listed in Table 2. The numbering schemes of all the studied molecules are similar to those of trimer and pentamer. The C atoms directly connected with N atoms donate more electrons and have larger positive charges. The other C and N atoms accept electrons and have negative charges, and H atoms have positive charges for the whole molecules. The benzene rings have positive charges and NH_2– (or –NH–) have negative charges. This shows that the transfers of π electrons occur on the chain connecting the benzene ring with N atom. Later, we will find that the largest contributions to the third-order polarizabilities originate from the conjugation and delocalization of π electron clouds along the chain direction. The calculated orbital energy gap E_g corresponding to the difference of the HOMO (highest occupied molecular orbital) and LUMO (lowest unoccupied molecular orbital) eigenvalues at the TDB3LYP ground state, and the first transition energy S_1 from the ground state to the first excited state, are listed in Table 3. It is found that the E_g and S_1 decrease with an increase of the conjugated lengths. After the number of repeat unit $N>5$, the values of E_g and S_1 go towards stabilization. The values of E_g and S_1 are 5.61 and 4.91 eV for monomer, and 3.84 and 3.34 eV for octamer, respectively. The different values of E_g between the N and $N-1$ (from $N=2$ to 8) are −0.92, −0.34, −0.21, −0.13, −0.07, −0.08 and −0.02 eV, and those of S_1 are −0.85, −0.30, −0.15, −0.11, −0.06, −0.07 and −0.03 eV,

Table 2
The calculated Mulliken population at the ground state for aniline oligomers

	Monomer	Tetramer	Heptamer
C1			
C2	0.3093	0.3038	0.3019
C3	−0.1730	−0.1773	−0.1774
C4	−0.1345	−0.1942	−0.1957
N1	−0.1390	0.3531	0.3561
H (C2)	−0.7878	−0.7884	−0.7879
H (C3)	0.1137	0.1167	0.1161
H (N)	0.1240	0.1188	0.1178
Ring–	0.3186	0.3161	0.3153
	0.1506	0.1930	0.1945
–Ring–		0.4185	0.4133
NH_2–	−0.1506	−0.1531	−0.1544
–NH_2–		−0.4576	−0.4599

Table 3
SOS||TDB3LYP/6-31G* average and chain axis component values (in 10^{-36} esu) of the static third-order polarizability, energy gap ($\Delta_{HOMO-LUMO}$)and the first excited energy of aniline oligomers

N	$\hbar\omega=0.0$ eV				$\hbar\omega=0.80$ eV				α	E_g (eV)	S_1 (eV)
	$\langle\gamma(3\omega)\rangle$	γ_{xxxx}	$\langle\gamma(\omega)\rangle$	γ_{xxxx}	$\langle\gamma(2\omega)\rangle$	γ_{xxxx}	$\langle\gamma(3\omega)\rangle$	γ_{xxxx}			
1	−0.014	0.32	−0.016	0.36	−0.019	0.36	0.007	0.47		5.64	4.91
2	1.235	9.88	1.870	13.37	2.183	14.98	4.045	24.19	5.68	4.69	4.06
3	2.110	19.48	5.510	37.36	7.264	46.36	18.862	104.72	7.79	4.35	3.76
4	8.929	44.61	18.201	91.27	23.341	116.43	58.83	290.89	3.55	4.14	3.61
5	35.293	175.3	54.905	273.44	66.476	330.61	144.577	717.20	4.04	4.01	3.50
6	52.682	246.3	86.648	410.49	106.814	507.06	249.395	1197.59	2.81	3.94	3.44
7	56.128	289.3	102.294	521.01	128.571	652.10	333.26	1671.92	2.16	3.86	3.37
8	63.41	309.8	120.190	587.91	151.093	737.94	407.26	1992.20	1.31	3.84	3.34

We also indicate the evolution of the power law dependence of γ as a function of chain length ($\gamma \propto N^{\alpha}$).

respectively. The obtained results show a strong length-dependence of E_g and S_1 for $N\leq 5$, and they are near a constant for $N>5$.

3.2. Third-order polarizabilities of aniline oligomers

For the calculation of γ, we generally truncate the infinite SOS expansion to finite one after apparent convergence of γ has reached. Fig. 2 shows the convergent behaviors of γ components with the largest contribution to the average third-order polarizabilities of $\langle\gamma\rangle$ at input photon energy of 0.80 eV for aniline oligomers. The largest contribution to the average third-order polarizability of $\langle\gamma\rangle$ is γ_{xxxx} (the most important component along the chain axis) from monomer to octamer, respectively. It is shown that the components of γ have converged after summations of 38 states for all studied species. The calculated value of γ_{xxxx} obtained from the 3rd state is nearly 100% of the γ_{xxxx} obtained from summation over 60 states for monomer, and the γ_{xxxx} obtained from the 5th state is 100% of the γ_{xxxx} obtained from summation over 60 states for dimmer, and the γ_{xxxx} obtained from the 6th state is 100% of the γ_{xxxx} obtained from summation over 60 states for trimer and tetramer, and the γ_{xxxx} obtained from the 7th, 8th, 9th and 9th state is 100% of the γ_{xxxx} obtained from summation over 60 states for pentamer, hexamer, heptamer and octamer, respectively. The calculated results indicate that the states after 40 have no contribution to third-order polarizabilities of all the studied species. Accordingly, it is a reasonable approximation in the calculation of γ by employing 60 states in the SOS method in this work.

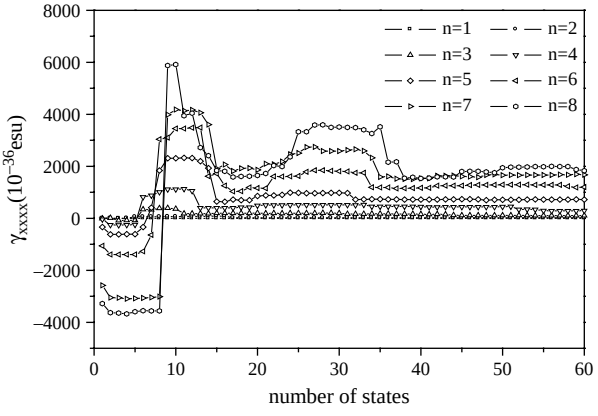

Fig. 2. Convergence behavior of $\gamma(-3\omega;\omega,\omega,\omega)_{xxxx}$ at input photon energy of 0.800 eV for aniline oligomers from monomer to octamer.

Now, we discuss the third-order optical properties based on the calculated results at the ground state of aniline oligomers. Fig. 3 depicts the frequent dependence of $\langle\gamma\rangle$ with different optical physical processes for dimer, pentamer and octamer of aniline, and the variation trends of other aniline oligomers are similar to those of the three aniline oligomers. At the static case when the input photon energy is zero, the values among the THG, EFISHG, DFWM processes have the same number, however, at the dynamic case when the input photon energy is 0.80 eV, the $\langle\gamma(3\omega)\rangle$, $\langle\gamma(2\omega)\rangle$, and $\langle\gamma(\omega)\rangle$ have different values for each aniline oligomer from repeat unit $N=2$–8, as listed in Table 3. The esu unit is taken for γ values in this work, which has the conversion relation with SI unit as $\gamma(\text{esu})=1.3982\times 10^{-14}\ \text{m}^5\ \text{V}^{-2}=1.2380\times 10^{-25}\ \text{C}^4\ \text{m}^4\ \text{J}^{-3}$ [32]. It is also

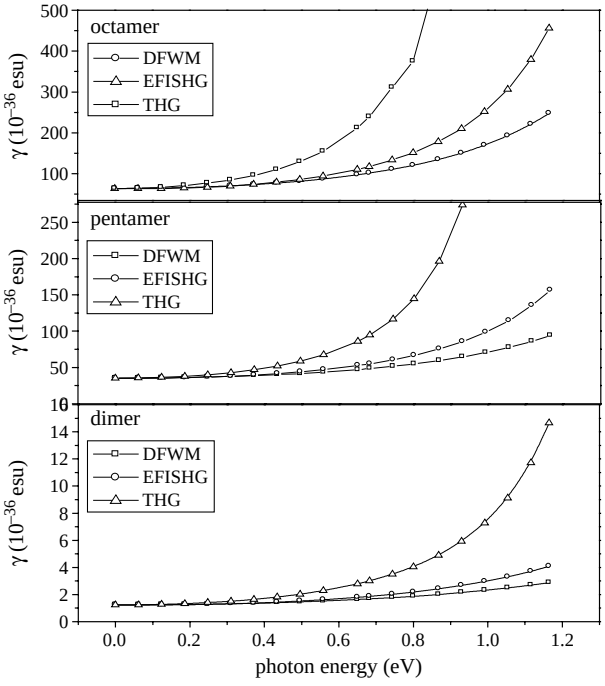

Fig. 3. The dynamic third-order polarizabilities of the THG, EFISHG and DFWM processes at ground state for dimmer, pentamer and octamer of aniline.

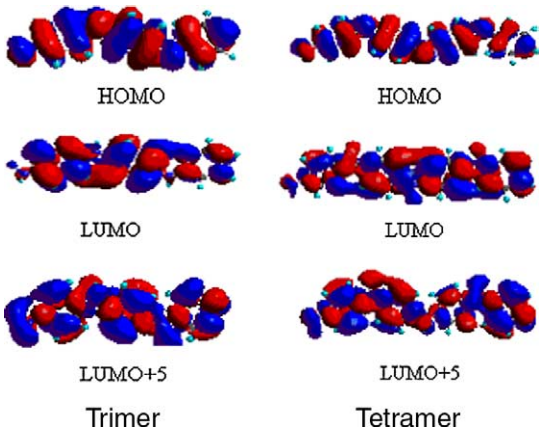

Fig. 4. The HOMO, LUMO and LUMO+5 of the aniline trimer and tetramer.

shown from Fig. 3 that the values of $\langle\gamma\rangle$ increase with the increasing of the input photon energy at the THG, EFISHG and DFWM processes. The first near resonant enhancement appears at about $\hbar\omega = 1.0$ eV for the THG process and the first near resonant enhancement does not appear even at $\hbar\omega = 1.165$ eV for the EFISHG or DFWM process. An analysis combining Fig. 2 with the calculated results of configuration interactions, we can find out what is the main contribution to the third-order polarizability. The 5th state of dimer has the greatest contribution from the configuration $\Psi_{49\rightarrow53}$, and this configuration is formed by electron transitions from the HOMO (the 49th orbital), composed of C-pπ and N-pπ orbitals, to the LUMO+3 (the 53th orbital) composed of C-pπ* orbitals. The 6th state of trimer and tetramer has the greatest contributions from the configurations $\Psi_{73\rightarrow78}$ and $\Psi_{97\rightarrow103}$, respectively. The configurations are formed by electron transitions from the HOMO composed of C-pπ and N-pπ orbitals to the LUMO+5 mainly composed of the C-pπ* orbitals. The situations of pentamer, hexamer, heptamer and octamer are similar to those of the trimer and tetramer. The states which have significant contributions to the γ_{xxxx} are formed by electron transitions from C-pπ and N-pπ orbitals to C-pπ* orbitals. The first excited state of all the studied aniline oligomers have the greatest contribution from the configuration which is formed by electron transitions from HOMO, composed of C-pπ and N-pπ orbitals, to the LUMO composed of C-pπ* and N-pπ* orbitals. Accordingly, we can say that the third-order polarizabilities of the all studied aniline oligomers are a significant contribution from the π to π* charge transfers. Fig. 4 gives the plots of the HOMO (orbital 73 of trimer and orbital 97 of tetramer), LUMO (orbital 74 of trimer and orbital 98 of tetramer) and LUMO+5 of the aniline trimer and tetramer, respectively. They represent the pictures of π-type orbital.

The saturation behavior of γ with the repeat units N is studied and the result is listed in Table 3 and visualized in Fig. 5. A strong length dependence of γ for $N<7$ is observed, and there appears at a much weaker length dependence of γ for $N\geq7$, where the band gap E_g becomes constant. To evaluate the saturation, we express the γ value as a function of a power of the chain length [33,34]:

$$\gamma \propto N^{\alpha(N)} \tag{3}$$

$$\log\gamma \propto \alpha(N)\log N \tag{4}$$

We find the average exponent value to be 3.30. Saturation is reached when the power value tends to 1. From Fig. 5, we can find that: (i) the γ response first pick up significantly with the extension of chain length, which means that the power value α strongly increases; (ii) the power value then enters a regime where it exists at a slow variation; for aniline oligomers, it is the case for the number of benzene rings of 3 and 6–7, and we calculate the power value in this regime to be around 3.5; (iii) the exponent in the power law starts decreasing around $N=7$–8, which indicates the beginning of the saturation regime. The power value α decreases to 1.31 for $N=8$. The above results are similar to those reported in previous studies on the third-order nonlinear optical response of oligothiophenes [6,19] and short polyenes [34]. The saturation of γ for $N>7$ may arise from electronic and conformational factors. Polarization and delocalization of π-electron along the molecular chain plays an essential role for $N<7$. With the increasing of N, as mentioned above, the configuration of aniline oligomer will be a large scroll and the conjugation length is limited. This leads to the reducing extent of conjugation and delocalization of π-electron, and it results in γ saturation for $N>7$ in the aniline oligomers.

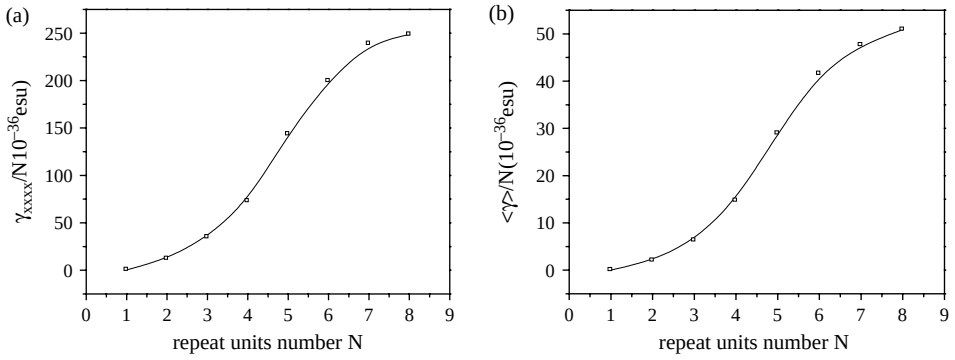

Fig. 5. Illustration of the evolution of the longitudinal γ_{xxxx} component (a) and the average value $\langle\gamma\rangle$ (b) per repeat units as a function of the repeat units number N at input photon energy 0.800 eV.

4. Conclusion

In this study, we have optimized the geometrical structure and calculated the dynamic third-order nonlinear polarizabilities γ at the ground states in the three optical process for aniline oligomers (from monomer to octamer).The optimized structures show that the benzene rings between neighbors are twisted and the configuration becomes large scroll along the molecular chain as the number of benzene ring are larger. The DFT or TDDFT calculations show that the HOMO-LUMO gaps E_g and the first excited energies S_1 decrease with the increase of repeated unit N, and they become constant when $N>7$. The SOS||TDDFT calculations show that the third-order polarizabilities increase with the increasing of the number of repeated units and the γ value approaches a saturation after $N>7$ in aniline oligomers. The saturation behavior of γ arises from conformational heterogeneity and limited conjugation length for aniline oligomers. It is predicted that a large scroll and broken π-configuration will determine the transition from nonlinear to thermodynamic behavior for organic oligomers.

Acknowledgements

This investigation was based on work supported by the National Natural Science Foundation of China under project 20373073, the Science Foundation of the Fujian Province (No. E0210028), and the Foundation of State Key Laboratory of Structural Chemistry (No. 030060).

References

[1] Chemla DS, Zyss J. Nonlinear optical properties of organic molecules and crystals, vols. 1 and 2. New York: Academic Press; 1986.
[2] Lawrence BL, Cha M, Torruellas WE, Stegeman GI, Etemad S, Baker G. Nonlinear Opt 1995;10:193.
[3] Samoc M, Samoc A, Luther-Davies B. Synth Met 2000;109:79–83.
[4] Ohnishi S, Gu FL, Naka K, Imamura A, Kirtman B, Aoki Y. J Phys Chem A 2004;108:8478–84.
[5] Wu DS, Cheng WD, Zhang H, Chen JT. Chem Phys Lett 2002;351: 486–94.
[6] Thienpont H, Rikken GLJA, Meijer EW, ten Hoeve W, Wynberg H. Phys Rev Lett 1990;65:2141–4.
[7] Beratan DN, Onuchic JN, Perry JW. J Phys Chem 1987;91:2696–8.
[8] Champagne B, Perpète EA, van Gisbergen SJA, Baerends E-J, Snijders JG, Soubra-Ghaoui C, et al. J Chem Phys 1998;109:10489–98.
[9] Champagne B, Perpète EA, van Gisbergen SJA, Baerends E-J, Snijders JG, Soubra-Ghaoui C, et al. J Phys Chem A 2000;104:4755–63.
[10] Lee AM, Colwell SM. J Chem Phys 1994;101:9704–9.
[11] Cohen AJ, Handy NC, Tozer DJ. Chem Phys Lett 1999;303:391–8.
[12] Van Faassen M, de Boeij PL, Van Leeuwen R, Berger JA, Snijders JG. J Chem Phys 2003;118:1044–53.
[13] Van Faassen M, de Boeij PL, Van Leeuwen R, Berger JA, Snijders JG. Phys Rev Lett 2002;88:186401.
[14] Zeng XR, Ko TM. Polymer 1998;39(5):1187–95.
[15] Kahol PK, Raghunathan A, McCormick BJ. Synth Met 2004;140: 261–7.
[16] Osaheni JA, Jenekhe SA, Vanherzeele H, Meth JS, Sun Y, MacDiarmid AG. J Phys Chem 1992;96(7):2830–6.
[17] Shuai Z, Brédas JL. Phys Rev B 1991;44:5962–5.
[18] Shuai Z, Brédas JL. Phys Rev B 1992;46:4395–404.
[19] Beljonne D, Shuai Z, Brédas JL. J Chem Phys 1993;98(11):8819–28.
[20] Zhao MT, Singh BP, Prasad PN. J Chem Phys 1988;89(9):5535–41.
[21] Humphrey JL, Lott KM, Wright ME, Kuciauskas D. J Phys Chem B 2005; 109:21496–8.
[22] Frisch MJ, Trucks GW, Schlegel HB, Scuseria GE, Robb MA, Cheeseman JR, et al. GAUSSIAN 98. Pittsburgh, PA: Gaussian Inc.; 1998.
[23] Becke AD. J Chem Phys 1993;98:5648–52.
[24] Orr BJ, Ward JF. Mol Phys 1971;20:513.
[25] Pierce BM. J Chem Phys 1989;91:791–811.
[26] Bauemschmitt R, Ahlrichs R. Chem Phys Lett 1996;256:454–64.
[27] Cheng WD, Wu DS, Zhang H, Li XD, Chen DG, Lan YZ, et al. J Phys Chem B 2004;108:12658–64.
[28] Li XD, Cheng WD, Wu DS, Lan YZ, Zhang H, Gong YJ, et al. J Phys Chem B 2005;109(12):5574–9.
[29] Fukuyo M, Hirotsu K, Higuich T. Acta Crystallogr, Sect B: Crystallogr Cryst Chem 1982;38:640.
[30] Boyer I, Quillard S, Corraze B, Deniard P, Evain M. Acta Crystallogr, Sect B: Crystallogr Cryst Chem 2000;56:e159.
[31] Evain M, Quillard S, Corraze B, Wang W, Macdiarmid AG. Acta Crystallogr, Sect E: Structure 2002;58:o343.
[32] Shelton DP, Rice JE. Chem Rev 1994;94:3–29.
[33] Brédas JL, Adant C, Tackx P, Persoons A, Pierce BM. Chem Rev 1994; 94:243–78.
[34] Shuai Z, Beljonne D, Brédas JL. J Chem Phys 1992;97:1132–7.